Supporting Information

Live-Cell Imaging of Single Receptor Composition Using Zero-Mode Waveguide Nanostructures

Christopher I. Richards[1,2], Khai Luong[3], Rahul Srinivasan[1], Stephen W. Turner[3], Dennis A. Dougherty[4], Jonas Korlach[3], and Henry A. Lester[1]*

1. Division of Biology 156-29, California Institute of Technology, 1200 East California Boulevard, Pasadena, CA 91125

2. Department of Chemistry, University of Kentucky, Chemistry-Physics Building, Lexington, KY 40506

3. Pacific Biosciences, 1380 Willow Road, Menlo Park, CA 94025

4. Division of Chemistry & Chemical Engineering 164-30, California Institute of Technology, 1200 East California Boulevard, Pasadena, CA 91125

*lester@caltech.edu

Detailed Methods and Analysis

Cell Culture

Mouse Neuro-2a (N2a) cells were cultured using standard techniques and maintained in Dulbecco's modified eagle medium (DMEM) supplemented with 10% fetal bovine serum (FBS). Cells were transfected with 500 ng of each nAChR plasmid. Cells were plated by adding 90,000 cells to poly-D-lysine–coated 35-mm glass-bottom imaging dishes (MatTek Corporation). After ~12 hr, plasmid DNA was mixed with cationic lipids by adding 500 ng of each nAChR plasmid

and 75 ng of plasma membrane localized monomeric cherry (PM-mcherry) plasmid to 4 µl of Expressfect transfection reagent in 200 µl DMEM. After 20 min at room temperature, the transfection mixture was added to Neuro-2a cells in 1 ml of plating medium and incubated at 37°C for 4 h. Dishes were rinsed twice with plating medium and incubated at 37 °C for 48 h.

Zero-mode waveguide arrays

Zero-mode waveguide arrays were prepared as described[1, 2]. ZMW arrays were fabricated from 100 mm diameter and 175 micron thick wafers of fused silica. After thorough cleaning the wafers were coated with a thin layer of aluminum (100 nm) via thermal evaporation. The samples were then spin-coated with electron-beam lithography resist and were then cured at 170° C. Wells were etched using an electron beam lithography system. Afterwards samples were thoroughly cleaned and prepared for glass coating. The ZMW array was then coated with a 4 nm thick layer of fused silica using atomic layer deposition. An array contains 45 panes, each composed of ~3100 ZMWs with X- and Y-spacing between wells of 1.3 and 4 µm. The diameter of the ZMWs is constant within a pane and varies monotonically from 85 to 200 nm across the array.

Excitation light at wavelengths greater than the cutoff wavelength (λc) where $\lambda c = 1.7d$ (d= well diameter) does not propagate through the ZMW. Instead an evanescent wave is formed at the entrance of the well. At the center of the well, (I) is equal to $e^{-z/L}$ (z = vertical position in the well, L = decay constant). This results in an effective penetration of 30-50 nm[3].

Preparation of N2a cells on ZMWs

Cells were cultured directly on unmodified glass coated ZMW arrays in custom culture dishes (supplementary figure 6)[4]. A volume of 100 µl of N2a medium (45% DMEM, 45% Optimem, 10% FBS) containing ~10,000 cells was plated onto the array surface. Samples were then placed at 37° C to allow cells to settle onto the arrays. We found this step crucial to obtain a relatively even distribution of cells across the entire array (Supplementary Figure 2). Afterwards 4 ml of medium was added to the dishes and they were stored at 37°C. After ~12 hr, plasmid DNA was mixed with cationic lipids by adding 500 ng of each nAChR plasmid and 75 ng of PM-mcherry plasmid to 4 µl of Expressfect transfection reagent in 200 µl DMEM. After 20 min at room temperature, the transfection mixture was added to Neuro-2a cells in 1.5 ml of plating medium and incubated at 37°C for 4 h. Dishes were rinsed twice with plating medium and incubated at 37 °C for 24 hours. In the case of cytisine and nicotine incubation, cells were rinsed with media containing 500 nM of the appropriate drug and left with the same final solution for 24 hr. All samples were imaged 24 hr after transfection.

Imaging Setup

Both a fiber coupled argon (488 nm) laser and a fiber coupled 561 nm laser were routed to the back port of an Olympus IX81 inverted microscope equipped with a zero drift control (ZDC2, Olympus) module (Supplementary Figure 6). Lasers were launched out of separate single-mode fibers along different optical paths. A planoconvex lens (f=100 mm) was placed in the path of

each laser ~ 10 cm from the fiber tip. The 488 nm beam was then aligned into the back port of the microscope while the 561 nm beam was aligned perpendicular to the path of the 488 nm laser. A mirror assembly was used to switch between illumination by the 561 nm or by the 488 nm beams. A second lens (achromatic doublet, f = 200 mm) was placed ~ 170 mm from the back aperture of a 100 X oil immersion objective (1.45 NA). The distance between the fiber launcher and the collimating lens was adjusted to focus the beam at the back focal plane of the objective. Via appropriate excitation and emission filters, fluorescence was directed to the side port of the microscope and focused on an electron-multiplying charge coupled device (EMCCD) camera (Andor iXon 897).

Data Collection and Analysis

Samples were separately excited with 200 W/cm^2 488 nm light for GFP and 200 W/cm^2 561 nm light for PM-mcherry. For α4β4, ZMWs with diameters of 144 nm and 200 nm were used for data analysis. These diameters generally gave measurable signals while recordable events were much less frequent for smaller diameters. For α4β2, 200 nm wells were used as they reliably gave signals while in the $\leq$ 144 nm wells these events were infrequently observed. Fluorescent wells were collected for individual panes of the array and data were pooled across these panes. As the data were collected using emission from the bottom of the array, individual cell boundaries were not delineated. During data collection mechanical and thermal drift was reduced with the internal ZDC2 module. Images were collected with an exposure time of 200 ms, preamplification gain of 5, and electron-multiplying gain of 190. The PM-mcherry marker was used to locate cells that had projected into the apertures by exciting with 561 nm light and scanning through each pane. As mcherry can be directly excited with 488 nm light, after a cell was identified the filter cube was changed to collect GFP fluorescence (excitation 488/10x and emission 515/30x) but not mcherry fluorescence. To reduce premature photobleaching, data acquisition was initiated prior to laser exposure, resulting in several dark frames at the beginning of each image stack. The shutter for the 488 nm laser was then opened during acquisition, ensuring that photobleaching did not occur during sample alignment or acquisition initiation.

The dark frames were removed from the image series and the remaining frames analyzed for each fluorescent well. Using Metamorph 7.7, we calculated the average background from a region of interest containing no fluorescent wells. This background was subtracted from each frame of the image stack. A circular region of interest (4 pixels in diameter) was selected and centered on each fluorescent well. The signal from each pixel within the region of interest was summed for each frame and the resulting value was used to plot intensity versus time traces. The resulting time trace was then visually inspected to determine the number of bleaching steps. Using only data exhibiting clearly defined fluorescence intensity levels, we calculated the number of bleaching steps. Traces showing unclear transitions were discarded (see Supplemental Figure 3).

Time trace selection and rejection

Assignment of the number of bleaching steps was performed by manual inspection of individual time traces. Approximately 20% of analyzed time traces exhibited clear bleaching steps such as

those shown in figures 3A and 3C. The observation of discrete levels of fluorescence and a clear transition between levels were the criteria for assignment of bleaching steps. Pentameric nAChRs assemble α and β subunits with a stoichiometry of either 3:2 or 2:3; there are two non-adjacent agonist binding sites at α-β subunit interfaces[5]. Because of the ambiguity in assigning stoichiometry using ensemble measurements we chose to restrict our analysis to those wells showing only single receptor signatures. Using these criteria we also discarded wells that showed ambiguous assignment of 3 versus 2 bleaching steps.

We measure plasma membrane resident receptors, so only fully assembled receptors and not individual subunits can be observed. Single step photobleaching would indicate the presence of one or more unlabeled subunits. These events most likely result from a combination of misfolded GFP molecules and the occurrence of unmeasured bleaching events. Some events presumably occur on a time scale unmeasureable in our experimental setup (<200 ms), and others occur near simultaneously with another bleaching event making them indistinguishable. Single-step photobleaching accounted for ~ 10% of the observed wells in studies of nAChRs. These events were discarded as they did not provide a way to distinguish between 3 versus 2 subunits. Control experiments of P2X2, which has 3 subunits, show that the majority of time traces with discernible bleaching steps yielded 3 discrete events (supplemental figure 4). Only a small percentage (15%) of the wells showed 2 bleaching steps. As P2X2 has a well-established homomeric assembly of 3 subunits this control experiment verifies that a small portion of the GFP-labeled subunits remain dark.

The majority (70%) of excluded wells were those that showed no steps during photobleaching. This is primarily due to time traces exhibiting an exponential decay as seen in supplementary figure 3A or those that had bleaching events obscured by fluorescence intermittency as seen in supplementary figure 3B. Despite exhibiting an exponential bleaching behavior that indicates multiple receptors, the time trace in supplementary figure 3A shows a fluorescence intensity that is approximately the same level seen for many time traces that show 3 clear bleaching steps. We believe that these signals result from multiple receptors that have not fully entered the well. As they are closer to the top of the well, they are excited at a lower intensity due to the exponentially decaying evanescent wave. Time traces that displayed this behavior were not measurable.

Wells that had blinking events that obscured transitions between steps (supplementary figure 3B) were also discarded. Assignment of the number of steps for these wells was ambiguous and no preference could be given for either 2 or 3 steps. A major concern for the rejection of these types of wells was whether blinking behavior would result in the preferential rejection of receptors containing either 2 or 3 GFP molecules. To address our concerns that blinking dynamics could introduce a bias in step assignment, we relied on our α4β4 experiments to test for differences in observed stoichiometry when separately labeling α and β subunits. The absence of a major shift in the observed stoichiometry (Figure 3) verifies the lack of bias in discarding undistinguishable

wells. Thus, we confined our measurements to those wells that exhibited definable 2 or 3 step events and view this as an accurate sampling of receptors on the plasma membrane.

In an attempt to determine our ability to observe more than 3 bleaching steps, studies were carried out on receptors composed of 5 identical α7-GFP subunits. These studies were limited by 2 factors: ZMW penetration was significantly reduced compared with other nAChRs; and wells populated with receptors exhibited only rare instances of discernible steps. Almost all time traces exhibited an exponential decay. These results show that we lose reliability in counting subunits beyond 3 steps. This appears to be primarily a function of the blinking dynamics and the intensity of individual GFP molecules within the environment created by the ZMW.

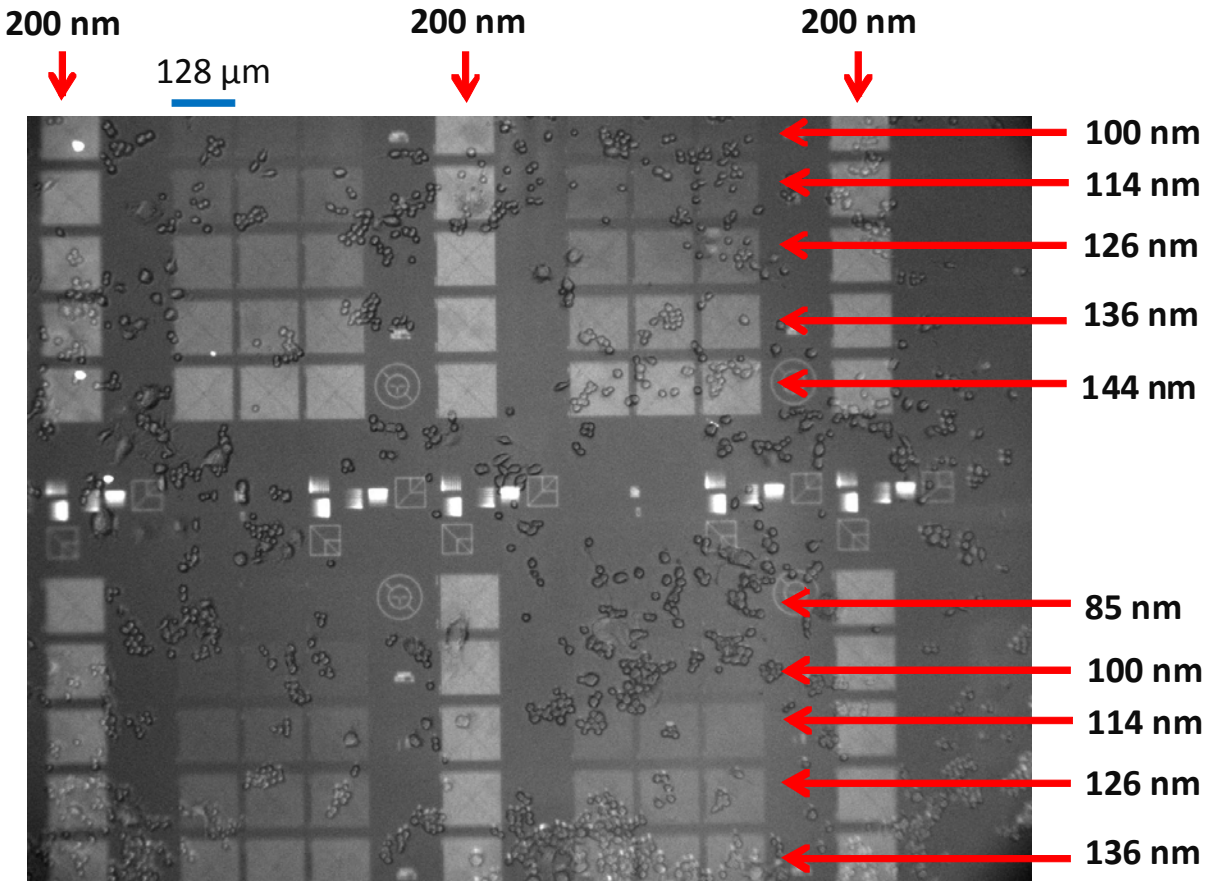

Supplementary Figure 1. *Cells on ZMW arrays*

Brightfield image of N2a cells plated on a ZMW array. Cells are distributed across the array. Each block contains panes of ZMWs ranging from diameters of 85 nm to 144 nm with additional 200 nm wells surrounding the panes. The differences in well diameter affect the transmission of light through the well where the smaller diameter results in reduced transmission.

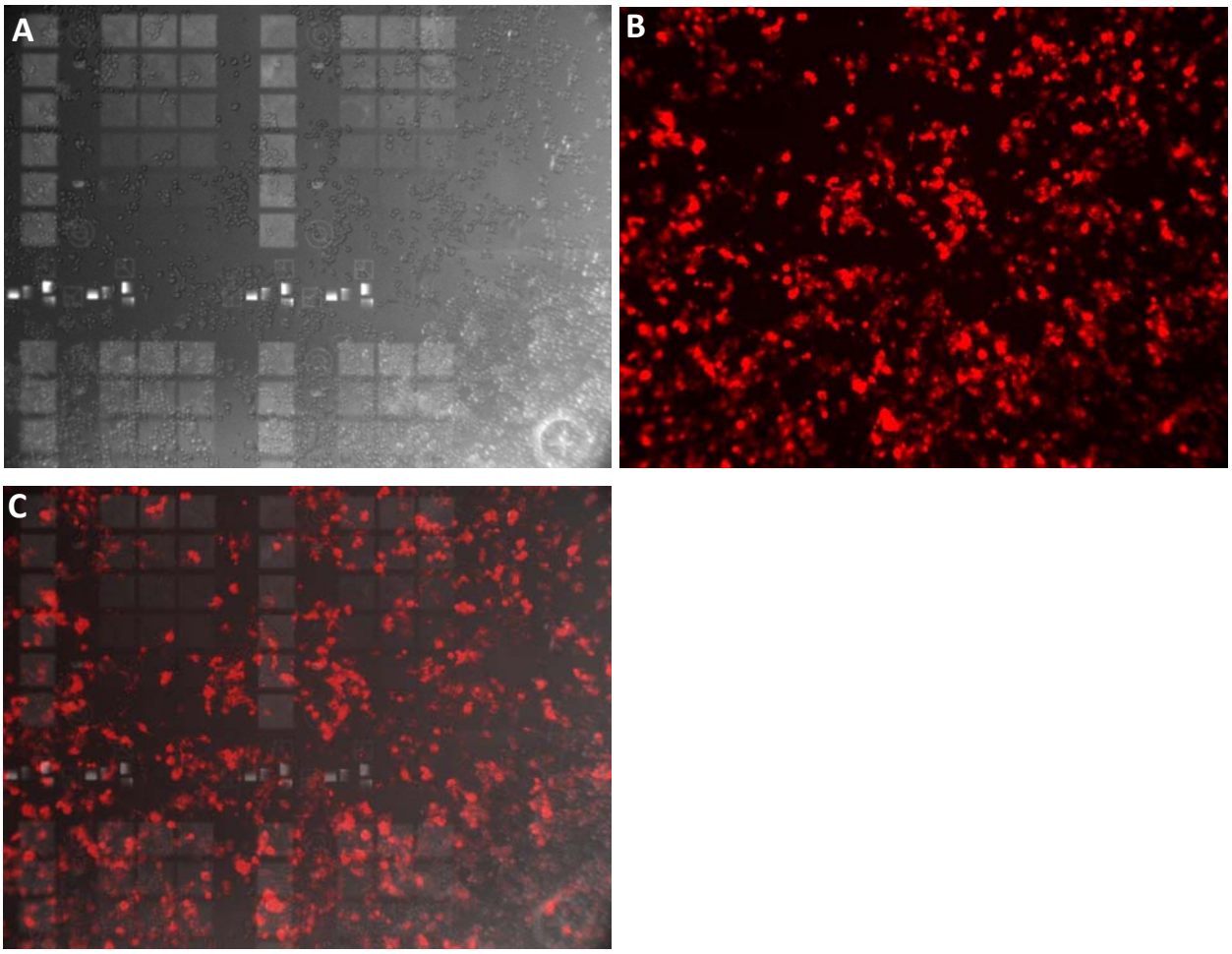

Supplementary Figure 2. *Fluorescent Cells on ZMW arrays*

A. Brightfield image of N2a cells plated on a ZMW array. Cells are distributed across the array. B. Fluorescent image of transfected cells on the ZMW array. C. An overlay of the fluorescent and brightfield images from A and C showing the distribution of fluorescent cells on the array panes.

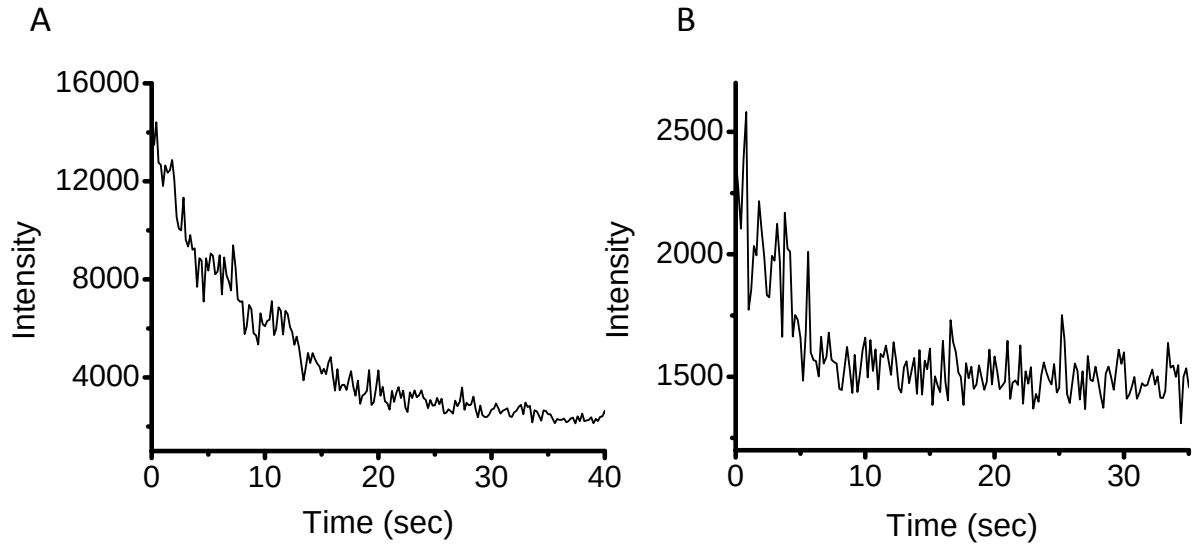

Supplementary Figure 3. *Time traces from uninformative wells*

A. Neuro2a cells plated on a ZMW array and transfected with α4-GFP β4-wt and the PM-mcherry marker. The array was excited with a 488 nm laser and the emission was filtered for the GFP signal. Both traces exemplify wells that exhibit uninformative fluorescent signals. **a.** A well exhibiting GFP fluorescence showing indistinct bleaching steps, indicating that the ZMW likely contains multiple receptors.

B. A well exhibiting GFP fluorescence complicated by fluorophore blinking dynamics, obscuring any bleaching steps.

Blinking Dynamics: Fluorescent proteins have been reported to blink on time scales ranging from microseconds to hundreds of milliseconds[6-8]. As individual molecules can often transition into a relatively long lived dark state, most time traces show temporary transitions from one discrete level to the other. Alternately when the molecule enters a prolonged dark state which is typically defined as a bleaching event, we sometimes see recovery from this event where the molecule becomes fluorescent for a short period of time. Both of these events are seen in time traces as either dips from the upper level to the lower or in spikes from the lower level back towards the upper. As the duration of these transient events is often of a similar time scale as our frame rate, the spikes do not always return fully to the previous level. Additionally, our experiments collect data on a time scale of 200 ms, thus events of similar duration can obscure clear transitions between steps. These cases complicate assignment of bleaching steps, as seen in supplementary figure 4B. In these uncertain cases, we have discarded these wells.

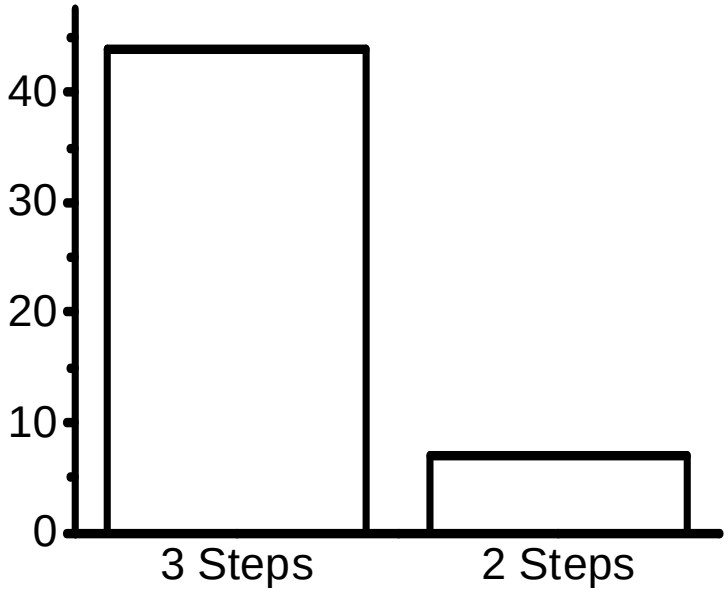

Supplementary Figure 4. *Bleaching steps of GFP labeled P2X2 trimers*

P2X2 receptors assemble as homomeric trimers. N2a cells plated on ZMW arrays were transfected with P2X2-GFP and excited with a 488 nm laser. Time traces from fluorescent wells were examined for observable bleaching steps and the occurrences of 2 and 3 bleaching steps were recorded. Approximately 85% of measurable wells exhibited 3 bleaching steps correlating to an assembled trimer as expected.

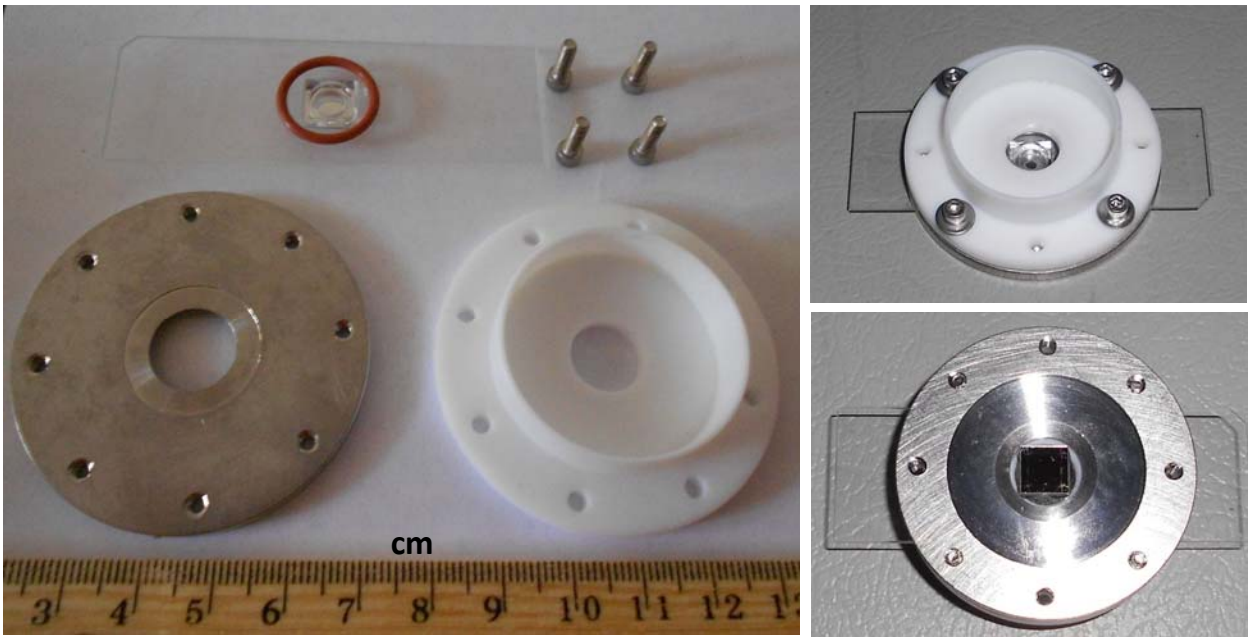

Supplemental figure 5. *Cell culturing and imaging apparatus*

a. The ZMW array is mounted to a glass slide in order to assemble the culture dish. The stainless steel base has a center hole (diameter = 13 mm) to allow access to the ZMW from the culture dish. The Teflon culture dish is fixed to the base with a silicone O-ring between the dish and the slide mounted ZMW.

b. A fully assembled culture dish showing sufficient volume to maintain cell health and to give access to the ZMW array.

c. Bottom view of the fully assembled showing the underside of the ZMW array and the beveled edge to accommodate the oil immersion objective.

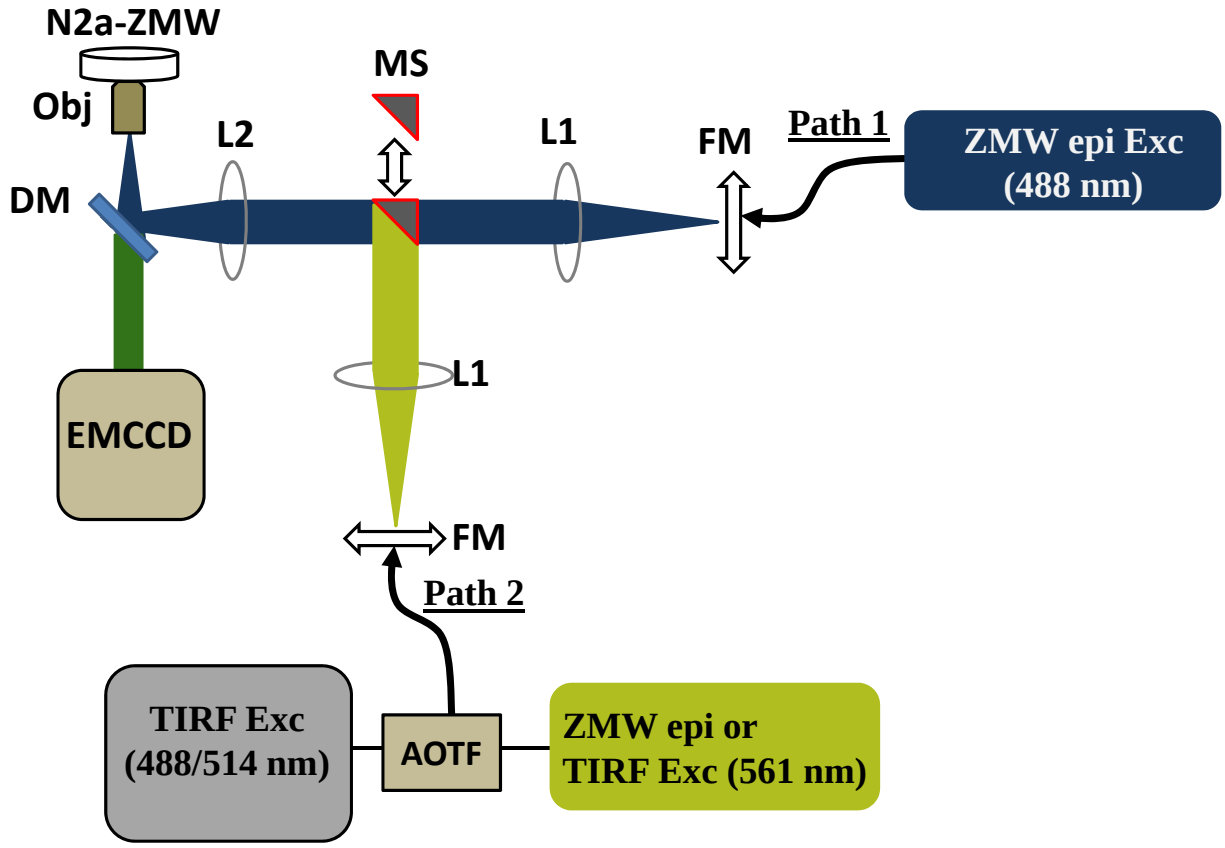

Supplemental figure 6. *Optical excitation and emission setup*

The 561 nm laser is controlled by the acousto-optic tunable filter (AOTF) and is used to illuminate PM-mcherry in both TIRF and ZMW based experiments (path 2). The 488 nm laser line (path 1) is used to illuminate the nAChR-GFP constructs for ZMW samples. TIRF excitation is achieved using the 488 nm laser in path 2. All lasers are fiber coupled (single mode 4 µm) and routed to a fiber mount (FM). The fiber mount is fixed to a stepping motor to allow for either TIRF or epi illumination. The fibers are also mounted on x, y, and z translatable stages for alignment purposes. The laser beam diverges out of the fiber and passes through a lens (L1; f = 100 mm) set 10 cm from the fiber mount. The lasers are then routed to a mirror assembly (MS) that can be slid in and out of the beam path to alternately allow the 488 nm laser to pass through (mirror out) or the 561 nm laser to reflect off (mirror in) to the back port of the microscope. A second lens (L2; achromatic doublet; f = 200 mm) is placed ~ 170 mm from the back aperture of a 100 X oil immersion objective (1.45 na). The excitation light is directed toward the objective with a dichroic mirror (DM). Emission light is then directed toward and collected with an EMCCD (Andor Ixon).

Atgggctgcatcaagagcaagcgcaaggacaacctgaacgacgacgaggccgccatgggctgcatcaagagcaagcgcaaggacaacctgaac
gacgacgaggcaccggtcgccaccatggtgagcaagggcgaggaggataacatggccatcatcaaggagttcatgcgcttcaaggtgcacatgga
gggctccgtgaacggccacgagttcgagatcgagggcgagggcgagggccgcccctacgagggcacccagaccgccaagctgaaggtgaccaag
ggtggccccctgcccttcgcctgggacatcctgtcccctcagttcatgtacggctccaaggcctacgtgaagcaccccgccgacatccccgactacttg
aagctgtccttccccgagggcttcaagtgggagcgcgtgatgaacttcgaggacggcggcgtggtgaccgtgacccaggactcctccctgcaggacg
gcgagttcatctacaaggtgaagctgcgcggcaccaacttcccctccgacggccccgtaatgcagaagaagaccatgggctgggaggcctcctccg
agcggatgtaccccgaggacggcgccctgaagggcgagatcaagcagaggctgaagctgaaggacggcggccactacgacgctgaggtcaagac
cacctacaaggccaagaagcccgtgcagctgcccggcgcctacaacgtcaacatcaagttggacatcacctcccacaacgaggactacaccatcgt
ggaacagtacgaacgcgccgagggccgccactccaccggcggcatggacgagctgtacaagtaa

Membrane localization
Linker
mCherry

Supplemental figure 7. *Structure of pmCherry*

The membrane localized mCherry marker contains the myristoylation signal sequence from Lyn kinase with the red fluorescing protein fused to the C-terminus.

References

1. Moran-Mirabal, J. M.; Craighead, H. G. *Methods* **2008,** 46, (1), 11-17.
2. Moran-Mirabal, J. M.; Torres, A. J.; Samiee, K. T.; Baird, B. A.; Craighead, H. G. *Nanotechnology* **2007,** 18, (19).
3. Levene, M. J.; Korlach, J.; Turner, S. W.; Foquet, M.; Craighead, H. G.; Webb, W. W. *Science* **2003,** 299, (5607), 682-686.
4. Wade, L. A. An Evanescent Perspective on Cells. California Insitute of Technology, Pasadena CA, 2010.
5. Miwa, J. M.; Freedman, R.; Lester, H. A. *Neuron* **2011,** 70, (1), 20-33.
6. Garcia-Parajo, M. F.; Segers-Nolten, G. M. J.; Veerman, J. A.; Greve, J.; van Hulst, N. F. *Proc. Natl. Acad. Sci. U. S. A.* **2000,** 97, (13), 7237-7242.
7. Dickson, R. M.; Cubitt, A. B.; Tsien, R. Y.; Moerner, W. E. *Nature* **1997,** 388, (6640), 355-8.
8. Schenk, A.; Ivanchenko, S.; Röcker, C.; Wiedenmann, J.; Nienhaus, G. U. *Biophys. J.* **2004,** 86, (1), 384-394.